SPACE PROPULSION 2018
BARCELO RENACIMIENTO HOTEL, SEVILLE, SPAIN / 14 – 18 MAY 2018

Endurance Testing of the STAR Additively Manufactured Resistojet

M. Robinson [(1)], A. Grubisic [(2)], F. Romei [(3)], C. Ogunlesi[(4)], S. Ahmed[(5)], P. Aimone[(6)], F. Dary[(7)], D. Gibbon[(8)]

(1,2,3,4,5) University of Southampton, University Road, Southampton, SO17 1BJ, United Kingdom
Emails of corresponding authors:
m.d.robinson@soton.ac.uk
a.grubisic@soton.ac.uk
(6,7) H.C. Starck Inc., 45 Industrial Place, Newton, MA, 02461, USA
(8) Surrey Satellite Technology Ltd., Tycho House, 20 Stephenson Road, Surrey Research Park, Guildford, Surrey, GU2 7YE, United Kingdom

KEYWORDS: resistojet, xenon, additive manufacture, spacecraft propulsion, endurance testing, life testing, all-electric

ABSTRACT:

This paper discusses the preliminary results of endurance testing of a resistojet thruster with a novel heat exchanger manufactured by selective laser melting. The heat exchanger consists of concentric thin walls which both recirculate the flow and act as a resistive element. A full assembly containing a prototype heat exchanger in 316L stainless steel was thermally cycled between operational temperatures in order to observe predicted failure modes. X-ray computed tomography scanning prior to and after the tests showed the nature of the primary failure mode as deformation of the concentric walls resulting in an electrical short.

1. INTRODUCTION

1.1. Project overview

The STAR (Super-high Temperature Additive-manufactured Resistojet) project at University of Southampton aims to develop a high-performance xenon resistojet, as an enabling technology for all-electric spacecraft based on a common inert propellant architecture for both the primary electric propulsion system and reaction control system. Such an architecture has been proposed by Coletti et al. [1], and the benefits of all-electric spacecraft are summarised by Grubisic and Gabriel [2].

Resistojets are a form of electrothermal rocket in which electrical power is used to directly heat a propellant via a heat exchanger. The heat exchanger can be directly or indirectly heated by electrical dissipation, subsequently heating the propellant. The propellant then underdoes gas dynamic expansion via a nozzle to generate a high-velocity exhaust jet.

Resistojets offer a performance advantage over cold gas thrusters, while being mechanically and electrically simple compared to other electric and chemical thrusters. They have a long history of use in multiple roles, for example station-keeping on Intelsat V, and orbit adjustment on the Iridium constellation [3]. Their characteristics make them well-suited to play a role in the emerging field of all-electric spacecraft. They are highly versatile, and can be used with many propellants. Low power resistojets can be powered directly from satellite regulated or unregulated bus voltage with no additional power processing, further reducing mass and complexity.

The specific impulse (I_{sp}) of a resistojet is largely determined by its temperature, as shown in Eq. 1, where C_p is the propellant constant-pressure specific heat capacity, T_0 is the stagnation temperature at the inlet to the nozzle, and the overall nozzle efficiency is captured by η_n [4]. Current commercially available resistojets such as the SSTL T50 are capable of temperatures up to 800 K, with a corresponding maximum I_{sp} of 48 s using xenon [5].

$$I_{sp} \approx \frac{\eta_n}{g_0}\sqrt{2C_pT_0} \qquad \text{Eq. 1}$$

The design requirement of STAR is to achieve a minimum of 80 s I_{sp} using xenon, corresponding to a minimum T_0 of 2400 K, with the aim of reaching 95 s I_{sp} at 3300 K. This will require the use of refractory materials in the thruster.

The current state of progress on STAR is summarised in [6]. Several prototype thruster assemblies have been produced using 316L stainless steel as a proof of concept for the design, and the use of additive manufacturing (AM). These thrusters are being tested to inform the development process of the next generation of the STAR. In parallel, the first STAR components manufactured using refractory materials are being analysed [7].

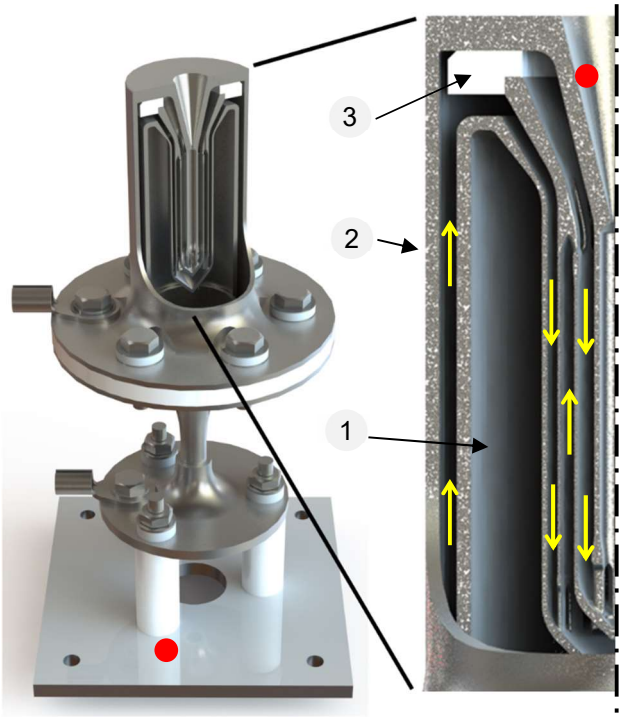

Figure 2: Cutaway of STAR prototype thruster assembly. 1 – AM heat exchanger/nozzle, 2 – pressure case, 3 – ceramic nozzle spacer. Yellow arrows indicate recirculating flow of propellant gas. Red dots indicate thermocouple positions.

1.2. Thruster design

The thruster under test is the prototype developed by Romei and Grubisic [4]. A schematic view of the design is shown in Fig. 2. The thruster consists of an AM heat exchanger/nozzle component, electron beam welded to an AM propellant inflow component at one end and a turned pressure case at the other, forming a hermetic seal. These components are all manufactured from 316L stainless steel. A nozzle spacer/support component manufactured from Macor ceramic serves a dual purpose of maintaining gas flow pathways through the heat exchanger and supporting the heating elements. A ceramic collar provides electrical isolation in the pressure case. The thruster is mounted to a test stand by three M3 screws on a 27 mm PCD, with ceramic sleeves and washers providing electrical and thermal isolation from the test stand/spacecraft.

The component of most interest in the endurance test of this paper is the AM integrated heat exchanger/nozzle. The component uses a concentric tube design, providing recirculating flow paths for both propellant gas and electric current, with the aim of maximising transfer of energy from electric input to heat in the propellant. The recirculating design achieves this by providing both a long gas residence time, and flowing gas from the outer radius towards the centre, thus providing some regenerative cooling of heated outer components. Fig. 2 indicates the gas flow.

1.3. Endurance requirements

The University of Southampton is working in collaboration with Surrey Satellite Technology Ltd (SSTL) to ensure the STAR project meets commercial performance and environmental test requirements. Target applications are for both auxiliary propulsion on an all-electric GEO telecommunications platform, and a primary propulsion system on a small LEO platform. The requirements for the latter are given precedence here, as this is the first anticipated use case.

The endurance requirement of the resistojet is determined by the thrust and total impulse requirements. The thruster must operate at a single thrust point within the range 20-50 mN, and must deliver a minimum of 23.5 kNs total impulse. This results in a minimum hot firing lifetime of 130-326 hours. The minimum anticipated firing time for the resistojet in a primary propulsion role is 5 minutes per manoeuvre.

2. METHODOLOGY

The test setup and methods are described in this section.

2.1. Test setup

Endurance tests for the STAR prototype were carried out in the David Fearn Electric Propulsion laboratory at the University of Southampton. The vacuum facility is shown in Fig. 1. It includes a large 2 m ø x 4 m vacuum chamber, with a smaller 0.75 m ø x 0.7 m “hatch” chamber that can be rapidly pumped down. The hatch chamber was used for endurance testing. Vacuum in the hatch chamber is provided by a Leybold TURBOVAC MAG W700 iP turbomolecular pump backed by an Edwards XDS 35i scroll pump with a speed of 40 m3h-1. Pressure in the chambers is monitored by a Pfeiffer Vacuum PKR 251 gauge with a Pirani sensor and an inverted magnetron cold cathode

Figure 1: David Fearn Electric Propulsion laboratory vacuum chamber at University of Southampton

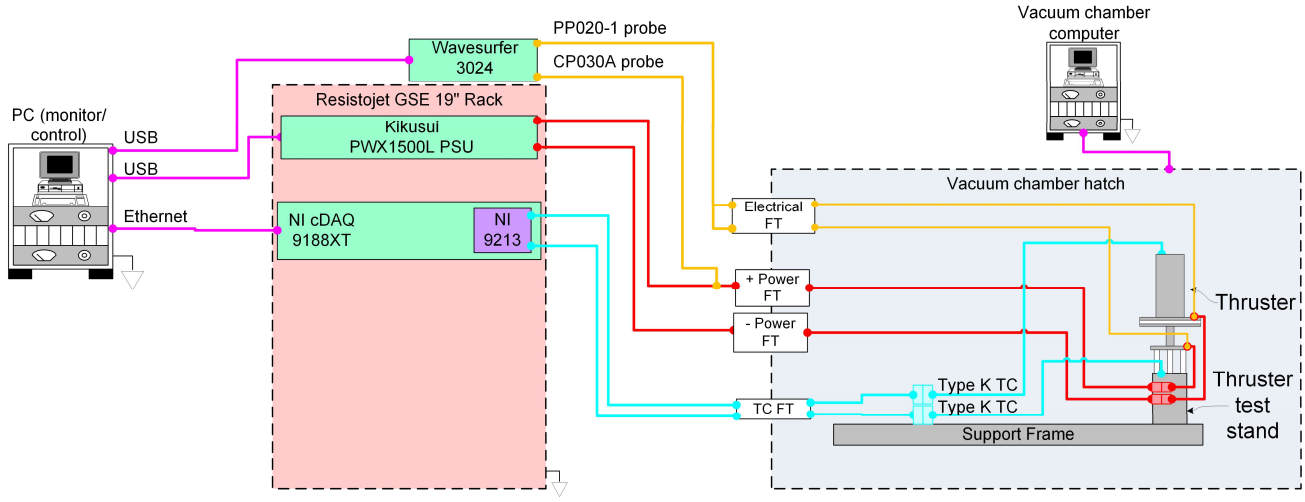

Figure 3: Endurance test setup schematic. Wire colours: purple – data connection, orange – oscilloscope measurement, red – power supply, blue – thermocouples.

gauge (combined measurement range 1000 – 5 x 10^{-9} mbar).

The thruster was provided with electrical power by a Kikusui PWX1500L power supply unit (PSU) operating in current-controlled mode. It was instrumented with two type K thermocouples, which were read out by a National Instruments NI-9213 input module, hosted in an NI cDAQ-9188XT CompactDAQ chassis. The positions of the thermocouples are shown in Fig. 2. The nozzle thermocouple was used to infer the temperature inside the resistojet, since the throat of the nozzle is too small to admit a thermocouple. The thermocouple placed at the base of the thruster isolation sleeves indicates the temperature at the spacecraft interface. The instrumented thruster assembly is shown in Fig. 4.

A Teledyne LeCroy Wavesurfer 3024 oscilloscope was used to measure current and voltage across the terminals of the resistojet, to calculate resistance and electrical power dissipation in the thruster. Two wires (Fig. 4 item 6) were connected between the terminals and a feedthrough. On the air side, a PP020-1 passive voltage probe measured the voltage between the terminals. A CP030A current probe measured current through the air side power cable from the PSU to the thruster.

A LabVIEW program controlled and monitored the resistojet during operation. The program uses an input file to generate a repeatable control sequence. During endurance testing, the PSU, thermocouple and oscilloscope measurements were collected by the LabVIEW program and output as a single log file.

A schematic of the test setup is shown in Fig. 3.

2.2. Test sequence

Endurance testing for the STAR consisted of repeated cycles of 5 minutes heating and 15 minutes cooling. During heating, the current supplied to the thruster was controlled at a constant 25 A, the maximum current used by Romei for performance testing of the STAR [8]. This current corresponds to ~25-28 W power as the thruster resistance changes with heating. During cooling, the current was reduced to 2 A. Since electric power is proportional to current squared, the power during the cooling period was less than 1 % of the heating power (<< 1 W), allowing the resistance of the thruster to be monitored as it cools while having a negligible effect on the cooling duration.

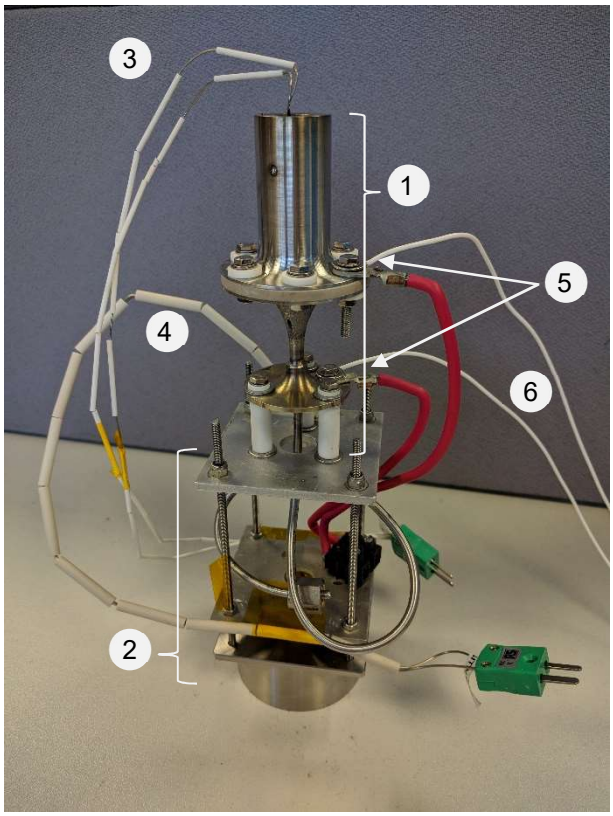

Figure 4: Resistojet assembly for endurance testing. 1 - thruster assembly, 2 - test stand, 3 - nozzle thermocouple, 4 - interface thermocouple, 5 - power terminals, 6 - voltage probe leads

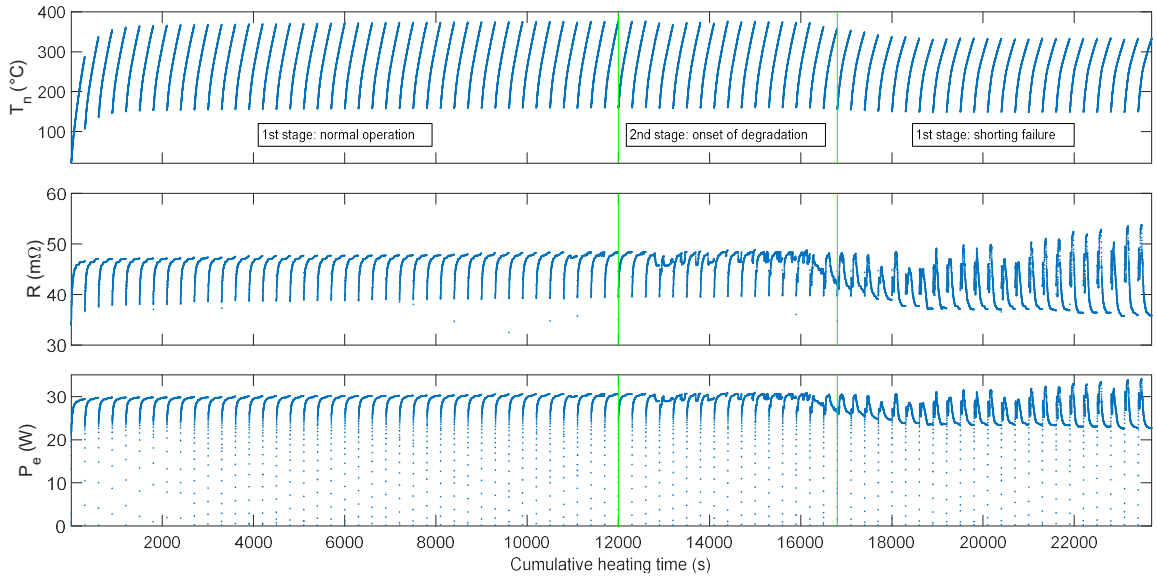

Figure 5: Endurance test overview (all 78 cycles) - cooling periods omitted for clarity

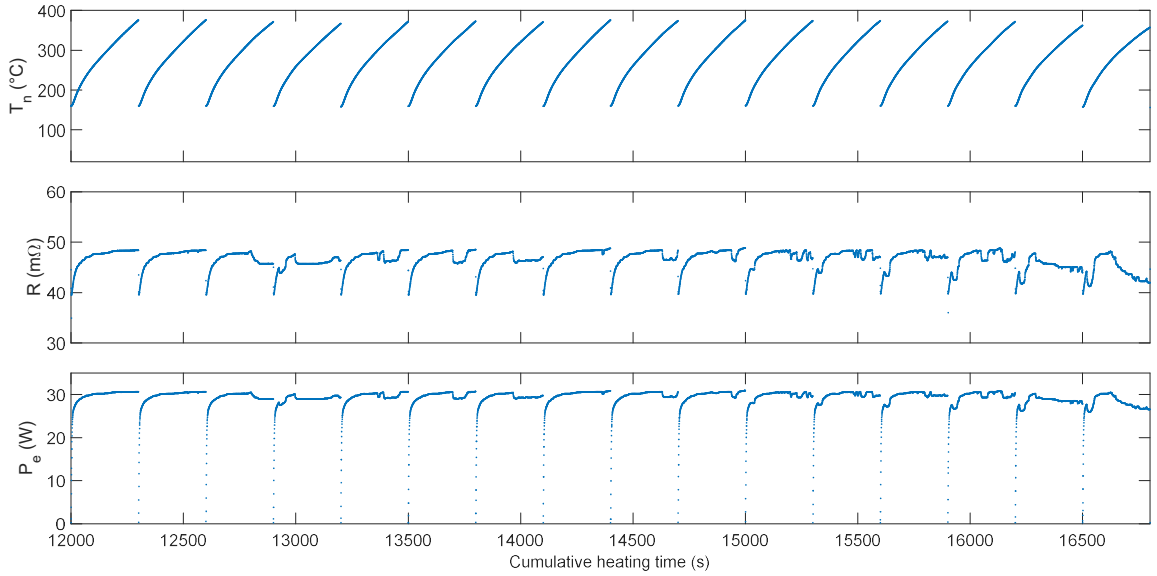

Figure 6: Endurance test second stage (onset of degradation) - cooling periods omitted for clarity

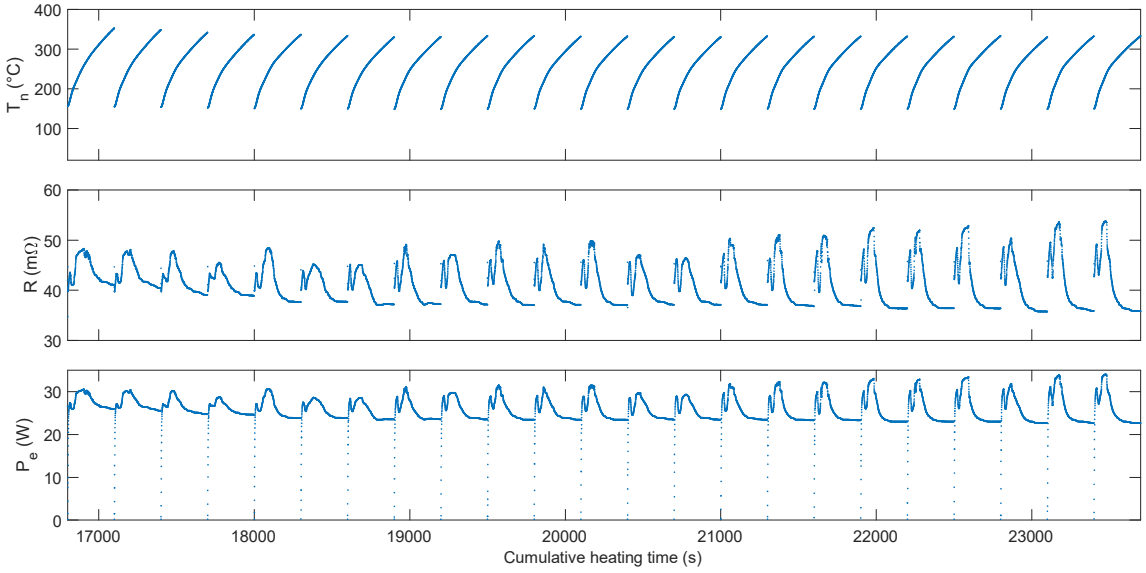

Figure 7: Endurance test third stage (shorting failure) - cooling periods omitted for clarity

No propellant was supplied to the thruster – due to the low operating pressure (4 bar, resulting in a maximum hoop stress less than 5 % of the 0.2 % offset yield strength of 316L), it was considered that degradation of the thruster during operation would most likely be caused by thermal distortion and fatigue.

The endurance test was carried out under vacuum to prevent oxidation of the hot structure and match the operational environment with regard to heat loss from the thruster. At the beginning of testing, the vacuum chamber pressure was 6.5 x 10^{-1} mbar. This was the maximum chamber pressure during the test.

During testing, the voltage and current across the resistojet terminals were measured and used to calculate the resistance. This was used to infer the condition of the thruster. Resistance is determined by the material, geometry and temperature of the thruster, hence if the measured resistance profile changes between cycles, it could indicate changes or degradation. For example, a sudden increase in resistance could indicate a crack, a sudden decrease could indicate contact between deforming components, or gradual changes could indicate plastic deformation or material loss.

Thermocouples captured the temperature at a point halfway along the diverging section of the nozzle and a point on the thrust stand at the base of the ceramic isolation sleeves (shown in Fig. 2). The nozzle temperature can be used to infer the maximum interior temperature of the resistojet according to a coupled electric/heat transfer model, as discussed in Section 4. The resistojet was cycled until evidence of failure was observed.

3. TEST RESULTS

The resistojet was cycled 78 times before being stopped due to an observed failure. The measurements are displayed in Figs. 5, 6 and 7. Note that, for clarity, the cooling periods are not shown. The upper trace of each figure shows temperature measured at the nozzle, T_n, the middle trace shows electrical resistance across the resistojet terminals, R, and the lower trace shows electrical power dissipated between the resistojet terminals, P_e.

Fig. 5 shows measurements taken from the resistojet during all 78 heating cycles of the test, plotted against cumulative heating time. Three distinct stages can be observed in Fig. 5, marked in the figure as normal operation, onset of degradation, and shorting failure.

The first stage, normal operation, begins with the resistojet heating from room temperature and lasts for approximately 40 cycles. In each cycle, the nozzle temperature increases, and the resistance

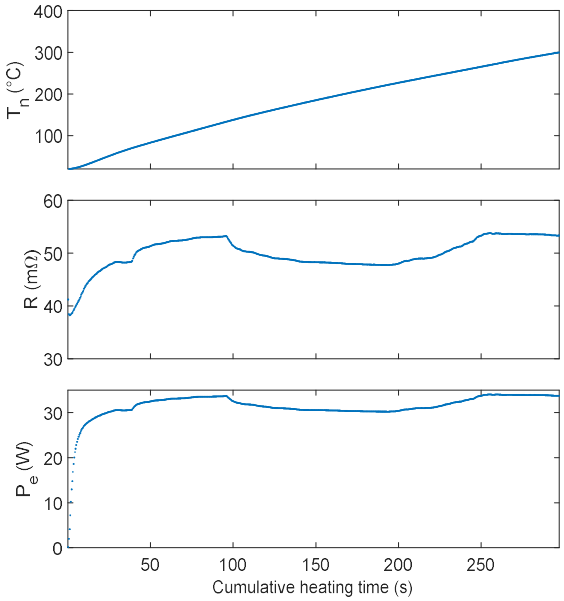

Figure 8: Single heating cycle from cold after life test.

increases as the thruster is heated, reaching a plateau at approximately 47 mΩ. The input power increases in direct proportion to the resistance, since the current is held constant. The temperature approximately reaches steady state within 5 cycles, with maximum (end of heating) and minimum (end of cooling) temperatures varying little thereafter. Resistance and power are highly repeatable, varying little after the first cycle. This may indicate that the core of the resistojet, inaccessible to direct temperature measurement, is heated more rapidly than the nozzle and at first the cycle time does not allow the nozzle to reach thermal equilibrium. The peak power during this stage is approximately 30 W.

In the second stage, onset of degradation, which lasts approximately 15 cycles, the resistance begins to deviate from the nominal profile described above. Fig. 6 shows this stage in more detail. Resistance and power appear to follow the same general trend shown during normal operation, with intermittent electrical short circuiting and a corresponding reduction in power (since current is constant). These vary in both duration and time of onset, but have similar magnitude reductions between 3-4 mΩ, corresponding to decreased power of approximately 2-3 W, approximately 10 % of the applied power. Since the power reduction is small, and the short circuits are generally brief, this does not have a large overall effect on the nozzle temperature. In later cycles with long-lasting short circuits, such as that at 13000 s, the peak temperature of the nozzle is visibly reduced.

In the third stage, the thruster appears to develop a more consistent short-circuiting behaviour. Fig. 7 shows this stage in more detail. In each cycle, the resistance initially increases as in normal operation. After approximately 20 s, the resistance rapidly drops to approximately the value at the start of the cycle, before continuing to rise due to further

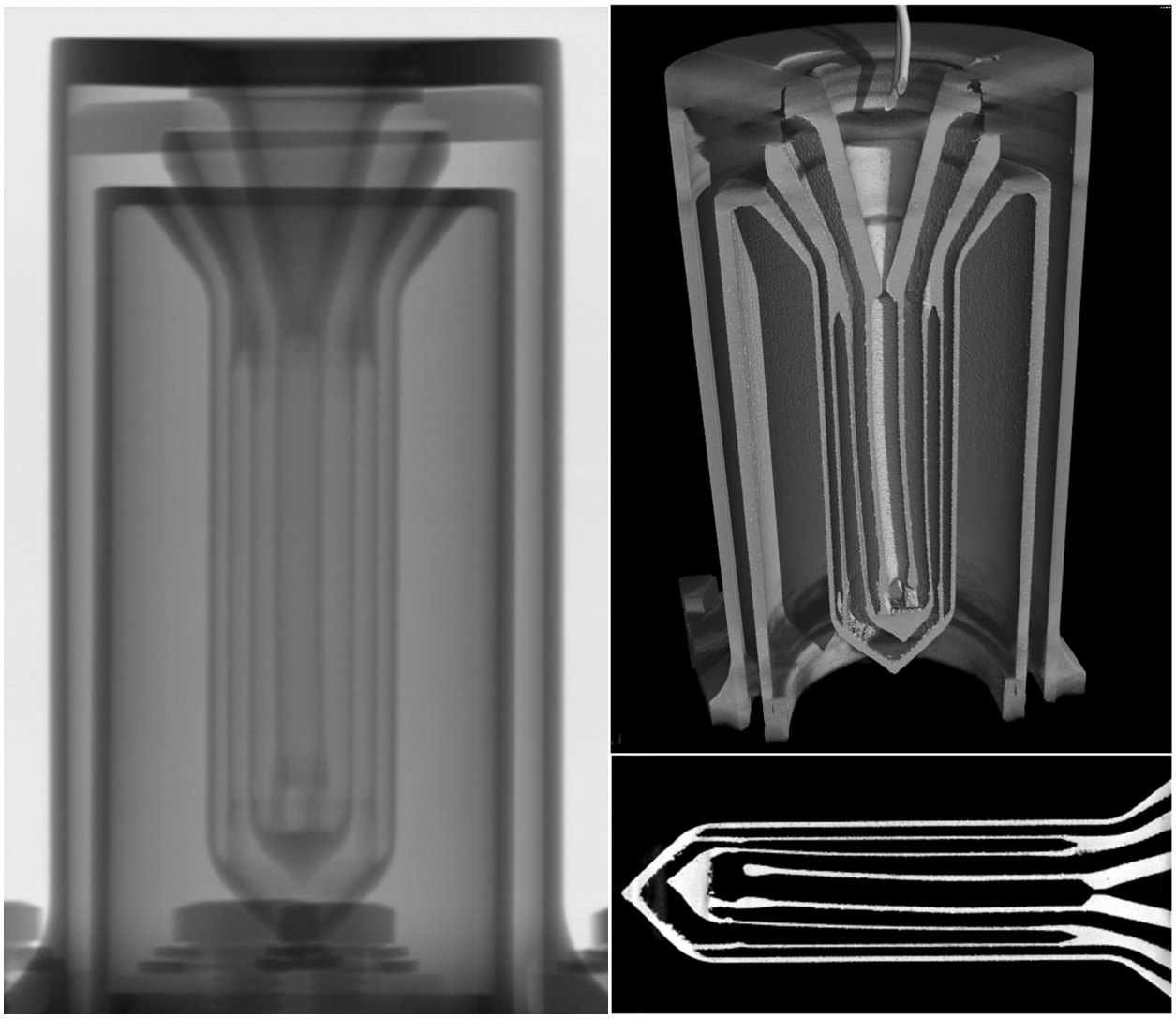

Figure 9: Left: x-ray radiograph of thruster following manufacturing, with straight centre tube (adapted from [4]*). Right: x-ray CT images of thruster following cycling, imaged while cold, with deformed centre tube. Top – 3D reconstruction of heat exchanger and case. Bottom – 2D slice focussing on heat exchanger.*

heating. After approximately 60 s another, greater decrease in resistance is seen, to a value approximately 5 mΩ below that at the start of the cycle. The changes in resistance follow a similar profile after the first 5-10 cycles of this stage, although the magnitude and sharpness of the resistance peak just before the major decrease does continue to vary.

The behaviour of the resistance in the third stage is consistent with electrical contact between two concentric tubes in the heat exchanger, creating a short circuit. The “double-dip” seems to indicate that an initial small contact is made between two parts of the heat exchanger, causing a small short, followed by a second contact being made as temperature, hence deformation, increases. The varying resistance profile at the onset of the large reduction may be the result of the rough surface of the AM material – this roughness can cause variable contact areas in each cycle due to asperities. As the temperature increases, the surfaces are more firmly contacted together, leading to the repeatable minimum resistance following the major decrease. The endurance test was monitored periodically, and was halted when the anomalous behaviour was discovered.

A single further heating cycle was performed after the thruster had fully cooled to room temperature, to investigate whether the thruster failure was permanent or transient. Fig. 8 shows the results of this cycle, in the same format as Figs. 5, 6 and 7. It shows similar behaviour to the second stage – an increasing resistance trend with intermittent shorting.

3.1. TEST ARTICLE ANALYSIS

Following 78 heating cycles, the endurance test was terminated due to the observed shorting behaviour. The thruster was visually inspected, and there were no outward indications of damage or degradation.

After cycling, the thruster was CT (Computed Tomography) scanned at the University of Southampton μ-VIS X-Ray Imaging Centre. A

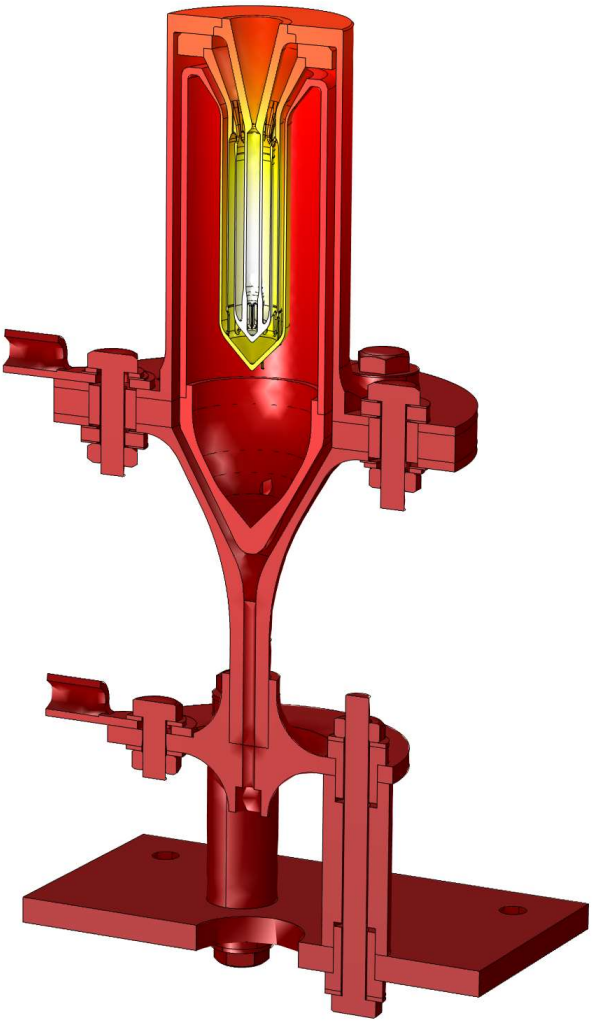

Figure 10: Example of electric/thermal model output for STAR prototype thruster. Yellow and white indicate hot regions, concentrated in the centre.

cross-section of the thruster, extracted from the CT scan data, is shown in Fig. 9. In the figure there is a clear deformation of the inner two cylinders of the heat exchanger. On the left hand side of Fig. 9 is a radiograph of the thruster prior to endurance testing [4]. In this image the inner cylinder is slightly bowed, but the second is straight and parallel to the third.

The thruster was scanned while cold, so the short circuit contact was not directly observed by the CT scan. However, it can be inferred that in each heating cycle, the inner tube bends and undergoes some permanent and some transient deformation. After a given number of cycles, as shown in the endurance test measurements, the permanent deformation is sufficient for the inner cylinder to contact the next outer cylinder when heated, causing a short circuit.

4. THERMAL MODELLING

A 3D coupled electric/thermal model of the STAR resistojet is under development by Romei as a continuation of previous efforts in multiphysics modelling of high-temperature resistojets [9][10]. This model was used to estimate the resistojet interior temperature, since the small throat of the resistojet prevents direct access to the interior.

Fig. 10 shows the temperature distribution of the electrothermal model after 280 s of heating at 25 A. The high temperatures are concentrated in the centre of the heat exchanger. The model indicates a temperature difference of approximately 500 °C between the thermocouple position in the nozzle, and the maximum temperature in the core. Applying this to the measured temperatures in the endurance test indicates a core temperature of over 800 °C.

Given the high predicted temperature inside the thruster, the deformation observed in the CT scan is unsurprising. 300 series stainless steels begin to soften and lose strength above approximately 500 °C, cooler than the maximum estimated temperature in the resistojet. In addition, the large thermal gradients (approximately 500 °C over 20 mm) may produce high thermal stresses. Previous concentric-tube high-temperature resistojet designs have incorporated design elements such as flexible bellows to provide stress-free thermal expansion [11], or ceramic microspheres as a mechanical support to prevent tubes bending and shorting [12]. The current STAR design does not incorporate such features.

5. CONCLUSIONS AND FUTURE WORK

The STAR project is ongoing, including further design efforts, and further work to characterise the environmental performance of the concept. Conducting the endurance test described herein has provided useful directions for design changes to improve the performance, cost, and manufacturability of the thruster.

The endurance test has elucidated a failure mode of the current design, in which the centre cylinder of the concentric heat exchanger can buckle off axis as it is cycled, eventually contacting the next cylinder and causing a short circuit. Knowledge of this failure mode will be used to improve the mechanical design in the next iteration. Although the material of the prototype thruster (316L) is very different to the refractory metals that will be used in future versions, the goal of the STAR project is to achieve the highest possible performance for a resistojet. Therefore problems of working close to a material's maximum working temperature are still likely to be present in the future, and the project will benefit from the knowledge gained from these early tests.

The tests have also demonstrated the effectiveness of using the electrical resistance as a means of investigating the failure modes of the resistojet. The resistance can be used to infer changes in the physical structure of the resistojet that arise from repeated operation. The availability of CT scanning

at the University of Southampton μ-VIS X-Ray Imaging Centre provided a valuable cross check of these inferences, allowing non-destructive imaging of the interior of the thruster.

6. ACKNOWLEDGEMENTS

This work was carried out as part of a PhD program funded through the Centre for Doctoral Training in Sustainable Infrastructure Systems, funded by the UK EPSRC (Engineering and Physical Sciences Research Council) under grant number EP/L01582X/1, and H.C. Starck GmbH. Additional funding was provided by the UK Space Agency, as part of the RADICAL (Refractory Additive Layer Manufacturing for Commercial Space Applications) project and the National Space Technology Program 2 via Innovate UK. The authors are grateful for the assistance of Dr. Kathryn Rankin and Dr. Mark Mavrogordato at the University of Southampton μ-VIS X-Ray Imaging Centre with non-destructive inspection, and for the assistance of Richard Dooler and Kevin Smith at the University of Southampton EDMC workshop in manufacturing the thruster.

7. REFERENCES

[1] M. Coletti, A. Grubisic, C. Collingwood, and S. Gabriel, “Electric propulsion subsystem architecture for an all-electric spacecraft,” INTECH, Feb. 2011.

[2] A. N. Grubisic and S. B. Gabriel, “Assessment of the T5 and T6 Hollow Cathodes as Reaction Control Thrusters,” *J. Propuls. Power*, vol. 32, no. 4, pp. 810–820, May 2016.

[3] W. A. Hoskins *et al.*, “30 years of electric propulsion flight experience at Aerojet Rocketdyne,” in *33rd International Electric Propulsion Conference*, 2013, pp. 1–12.

[4] F. Romei, A. N. Grubišić, and D. Gibbon, “Manufacturing of a high-temperature resistojet heat exchanger by selective laser melting,” *Acta Astronaut.*, vol. 138, pp. 356–368, 2017.

[5] D. Nicolini, “Xenon Resistojets as Secondary Propulsion on EP Spacecrafts and Performance Results of Resistojets Using Xenon,” *Proc. 28th Int. Electr. Propuls. Conf. Toulouse, Fr. 2003*, 2003.

[6] F. Romei, A. N. Grubisic, and D. Gibbon, “High performance resistojet thruster: STAR Status Update,” in *Space Propulsion 2018*, 2018.

[7] C. Ogunlesi *et al.*, “Novel Non-Destructive Inspection of the STAR Additively Manufactured Resistojet,” in *Space Propulsion 2018*, 2018.

[8] F. Romei, A. Grubisic, and D. Gibbon, “Performance testing and evaluation of a high temperature xenon resistojet prototype manufactured by selective laser melting,” 2017.

[9] F. Romei, A. Grubisic, D. Lasagna, and D. Gibbon, “Multiphysics model validation of resistojets with concentric tubular heat exchanger,” in *7th European Conference for Aeronautics and Space Sciences (EUCASS 2017)*, 2017.

[10] F. Romei, A. Grubisic, D. Gibbon, O. Lane, R. A. Hertford, and G. Roberts, “A Thermo-fluidic Model for a Low Power Xenon Resistojet,” Jul. 2015.

[11] C. R. Halbach and R. Y. Yoshida, “Development of a Biowaste Resistojet,” *AIAA J. Spacecr.*, vol. 8, no. 3, pp. 273–277, 1971.

[12] D. G. Philips, “Technology Development of a Biowaste Resistojet Volume II,” 1972.